The Role of Dissolved Gas in Ionic Liquid Electrolytes for Secondary Lithium Metal Batteries

*Johanna K. Stark[1], Yi Ding[2], and Paul A. Kohl[1,]**

[1]Georgia Institute of Technology

School of Chemical and Biomolecular Engineering

Atlanta, GA 30332-0100 USA

[2]US Army RDECOM-TARDEC

AMSRD-TAR-R, MS 159

6501 E. 11th Street

Warren, MI 48397-5000

*kohl@gatech.edu

Keywords: lithium metal, anode, ionic liquid

Report Documentation Page

Form Approved
OMB No. 0704-0188

1. REPORT DATE	2. REPORT TYPE	3. DATES COVERED
07 JAN 2013	**Journal Article**	**22-04-2012 to 25-11-2012**

4. TITLE AND SUBTITLE
The Role of Dissolved Gas in Ionic Liquid Electrolytes for Secondary Lithium Metal Batteries

5a. CONTRACT NUMBER
5b. GRANT NUMBER
5c. PROGRAM ELEMENT NUMBER

6. AUTHOR(S)
Johanna Stark; Yi Ding; Paul Kohl

5d. PROJECT NUMBER
5e. TASK NUMBER
5f. WORK UNIT NUMBER

7. PERFORMING ORGANIZATION NAME(S) AND ADDRESS(ES)
Georgia Institute of Technology,School of Chemical and Biomolecular Engineering,225 North Ave,Warren,Mi,48397-5000

8. PERFORMING ORGANIZATION REPORT NUMBER
; #23591

9. SPONSORING/MONITORING AGENCY NAME(S) AND ADDRESS(ES)
U.S. Army TARDEC, 6501 East Eleven Mile Rd, Warren, Mi, 48397-5000

10. SPONSOR/MONITOR'S ACRONYM(S)
TARDEC

11. SPONSOR/MONITOR'S REPORT NUMBER(S)
#23591

12. DISTRIBUTION/AVAILABILITY STATEMENT
Approved for public release; distribution unlimited

13. SUPPLEMENTARY NOTES
journal of physical chemistry

14. ABSTRACT
The effect of dissolved gas on the reversibility of a Li/Li+ electrode in an ionic liquid electrolyte was investigated. Lithium metal is a potential anode in lithium batteries. The ionic liquid electrolyte was saturated with argon, nitrogen, oxygen, air, or carbon dioxide and the coulombic efficiency for the reduction and reoxidation of lithium metal was measured. Secondary ion mass spectroscopy (SIMS) was used to determine the thickness and composition of the solid electrolyte interphase (SEI) layer formed on the lithium metal. The coulombic cycling efficiency was highest with oxygen, nitrogen, and air. The coulombic efficiency was significantly lower with dissolved carbon dioxide. SIMS revealed that the SEI layer was made up of primarily LiF regardless of the gas used. The thickness of the SEI layer was the main determinant of cycling efficiency. A thinner SEI, observed with nitrogen and oxygen, lead to the highest coulombic efficiency, whereas, carbon dioxide produced a thick SEI which appeared to inhibit lithium deposition.

15. SUBJECT TERMS
lithium metal, anode, ionic liquid

16. SECURITY CLASSIFICATION OF:			17. LIMITATION OF ABSTRACT	18. NUMBER OF PAGES	19a. NAME OF RESPONSIBLE PERSON
a. REPORT	b. ABSTRACT	c. THIS PAGE			
unclassified	**unclassified**	**unclassified**	**Public Release**	**23**	

ABSTRACT

The effect of dissolved gas on the reversibility of a Li/Li^+ electrode in an ionic liquid electrolyte was investigated. Lithium metal is a potential anode in lithium batteries. The ionic liquid electrolyte was saturated with argon, nitrogen, oxygen, air, or carbon dioxide and the coulombic efficiency for the reduction and reoxidation of lithium metal was measured. Secondary ion mass spectroscopy (SIMS) was used to determine the thickness and composition of the solid electrolyte interphase (SEI) layer formed on the lithium metal. The coulombic cycling efficiency was highest with oxygen, nitrogen, and air. The coulombic efficiency was significantly lower with dissolved carbon dioxide. SIMS revealed that the SEI layer was made up of primarily LiF regardless of the gas used. The thickness of the SEI layer was the main determinant of cycling efficiency. A thinner SEI, observed with nitrogen and oxygen, lead to the highest coulombic efficiency, whereas, carbon dioxide produced a thick SEI which appeared to inhibit lithium deposition.

Introduction

The ubiquity of mobile electronics has spurred interest in high energy density secondary batteries. Cell phones, laptops, and music players gain their strengths from being portable devices, but long lasting batteries with good cycleability must be developed to support the increasing need for energy.

Currently, these devices use lithium-ion batteries comprised of a graphite anode and metal oxide cathode. Lithium, being the third-lightest element, is already synonymous with high energy density batteries. Its low molecular weight makes it the lightest active material for batteries. The structures and materials that support shuttling lithium ions (battery cycling) such as the separator, electrolyte, and cathode and anode superstructures contribute most of the weight of the battery. To eliminate this bulk, researchers have looked at higher energy density electrodes such as silicon and lithium-metal anodes. Lithium metal anodes present an interesting opportunity because they completely eliminate the anode superstructure material. The active material, extremely light lithium metal, is used directly as the anode. The lithium anode could also be potentially cycled at higher rates because there would be no diffusion limitation within the anode; the active material is perpetually on the surface. This lithium metal anode represents the upper bound for anode energy density.

A lithium metal anode faces two principal challenges: the formation of a stable solid electrolyte interface (SEI) and the ability of electro-deposit lithium non-dendritically. When lithium is electrodeposited, as during battery charging, it tends to form needle-like structures or dendrites. These protrusions are a concern for batteries because they can cause short-circuit the two electrodes and cause the battery to fail. Work has focused on physically containing the anode with a hard polymer or ceramic separator.[1] This can prevent dendrites from shorting the cell but

does not solve the problem on a fundamental level. Additives have been shown to alter plating in lithium, including the appearance of dendrites, but a smooth deposit has not been achieved.

Because of lithium's reactivity, the formation of a stable SEI is imperative to prevent the irreversible reaction between lithium and the electrolyte. On a graphite anode, the SEI is supported on the graphite surface while the lithium ions intercalate into the bulk. The SEI on graphite is usually formed with the help of additives within the electrolyte. Cyclic carbonates, such as ethylene carbonate and vinylene carbonate, are thought to undergoing reduction and ring-opening on the surface of the electrode.[2–7] The SEI on the surface of the lithium metal must form directly on the active material, which is more difficult than a host-type anode due to the dissolution of metal surface upon oxidation during cycling. Vinylene carbonate and other additives have been successfully used as SEI forming agents but have not completely solved the lithium anode stability problem.[8–10]

In this study, dissolved gases were investigated for their role in forming the SEI on the metal surface. Lithium batteries can be assembled in the absence of ambient water vapor (i.e. dry rooms) where the electrolyte is saturated with air.[7,10–12] Gases dissolve in the electrolyte in small amounts and can thus be used the affect the SEI in controlled ways.

Electrolytes for a lithium metal anode include ceramic separators, polymer membranes[13], organic electrolytes[14–16], and ionic liquids[17–19]. Ionic liquids are interesting because they are stable over a wide potential range, making them good candidates for future high-voltage batteries. Ionic liquids are also advantageous in terms of battery safety because they have near zero low vapor pressure and are generally nonflammable. Ionic liquids used to deposit lithium metal include pyrolidinium, pyrridinium, and quaternary ammonium ionic liquids.

Trimethylbutylammonium bis(triflouromethanesulfonyl)imide (N_{1114}-Tf_2N) ionic liquid is used in this study because it has high coulombic efficiency for the reduction and reoxidation of lithium metal has shown reversible lithium deposit and was used in this work[18,20,21]. Ionic liquids have also received attention as carbon dioxide capture mediums. In particular, researchers have investigated imidazolium-based ionic liquids for CO_2 capture because of the high solubility of CO_2. Data comparing CO_2, N_2, and O_2 solubility in ionic liquid have been reported.[22–26] In battery applications, soluble gases can be used to deliver small amounts of potentially SEI forming reactants. N_2 and O_2 can both react with lithium and be potential components of the SEI. The effect of dissolved gas on the lithium metal SEI and cycling efficiency are investigated in this study.

Experimental Methods

A liquid electrolyte (compared to a ion conducting solid electrolyte) was chosen for this study because intimate contact is required between the lithium metal and the electrolyte during the changing surface area events of lithium deposition and oxidation. Trimethylbutylammonium bis(triflouromethanesulfonyl)imide (N_{1114}-Tf_2N, 99%, Iolitec), Figure 1, and lithium bis(triflouromethanesulfonyl)imide ($LiTf_2N$, 99%, Acros) were mixed to give a 1M Li^+ electrolyte. The electrolyte was dried under vacuum for at least 15 h before use.

A beaker-cell with connections for two electrodes and a gas port was constructed for maintaining the ionic liquid under saturated conditions with each of the gases during the electrochemical cycling experiments. The ionic liquid was taken from vacuum line into an argon filled glovebox and transferred into the modified beaker cell for experimentation. The gas port

allowed for bubbling of a test gas before starting the electrochemical experiments. During the electrochemical experiments, the head space above the ionic liquid was maintained with the same test gas to avoid contamination from the ambient air. A second cell of similar design was used to for the experiments under vacuum. The vacuum cell had ground glass joints and vacuum tight electrical feedthroughs. The cell was leak tested with a helium lead detector before use.

A stainless steel type 316 working electrode and lithium counter/reference electrode were used for the electrochemical cycling experiments. First, excess metal (1 C/cm^2) was deposited on the stainless steel at 0.1 mA/cm^2. Then, 10% of the initial lithium capacity was cycled at 0.1 mA/cm^2 on each cycle until the lithium was exhausted during the oxidation part of the cycle. That is, 0.1 C/cm^2 of lithium was deposited and then 0.1 C/cm^2 of lithium was oxidized during each cycle. The potential was recorded during the constant current reduction and oxidation portions of the cycle, as shown for example in Figure 2. When there was no longer adequate lithium metal for the oxidation step, the potential rose sharply and the experiment is terminated. The number of cycles was recorded and the total charge for deposition and oxidation was used to give an average coulombic efficiency for the lithium deposition and stripping process. This cycling method avoided stripping the lithium metal from anode to the bare stainless steel substrate during each cycle. If the lithium were stripped to the stainless steel substrate, the SEI layer would likely be destroyed or at least changed on each cycle. Also, the iterative cycling method more closely mimics a real battery that would contain excess active material.

Time of flight secondary ion mass spectroscopy (ToF SIMS) was used for depth profiling and chemical analysis of the SEI. The same experimental set-up was used to prepare the ToF SIMS samples as described above: 1 C/cm^2 lithium deposition on a 316 stainless steel electrode. The sample gently washed in DMC in the glovebox before SIMS analysis. Samples were

analyzed with an ION-TOF5 SIMS using bismuth as the primary ion. Depth profiling was done by sputtering the samples using 500 keV cesium ions over a 500 x 500 µm area. The analysis area was 150 x 150 µm within the larger sputtered area.

Results and Discussion

Ionic liquids absorb ambient gas from the surroundings, but can be degassed by placing them in vacuum. The absorbed gas can usually be observed as bubbles leaving the liquid. In this work, the ionic liquid was saturated with specific gases to determine their effect on SEI formation and the coulombic efficiency of Li cycling. The gases evaluated include argon, oxygen, nitrogen, dry air, and carbon dioxide.

Experiments were performed to ensure that the ionic liquid was saturated with gas. A 1M Li^+ ionic liquid electrolyte was bubbled with nitrogen gas for 15 min, 3 h, and 6 h followed by measurement of the cycling efficiency. After the initial bubbling period, the gas of interest was maintained in the head space of the cell so that the electrolyte would be blanketed with the proper gas during the experiment. The electrolyte was allowed to settle for 10 min before the cycling experiment began. The coulombic efficiencies calculated from these experiments are shown in Figure 3.

The coulombic efficiency using argon gas, 75%, was used as a reference. Argon was chosen as a reference because it is not reactive with lithium metal. After a 15 min nitrogen bubbling, the coulombic efficiency increased slightly compared to the argon reference. A longer nitrogen bubbling time, 3 h and 6 h, led to higher coulombic efficiency values, however, no further improvements were observed with longer bubbling times. These results indicate that the time

required for the electrolyte to saturate and equilibrate with the ambient is about 3h. Each subsequent experiment was started with the cell assembled in the argon glovebox and the same saturation time of 3 h was used for each gas.

Figure 4 shows the coulombic efficiency for lithium with different gases bubbled for 3 h prior to the experiment. Argon is unreactive with lithium. Nitrogen may form lithium nitride (Li_3N) and oxygen may form lithium oxide (Li_2O) on the lithium metal surface. The vacuum experiment was conducted as a control since little or no gas should be present in the system. The experiments under vacuum and argon yielded similar coulombic efficiencies. The similarity between argon and vacuum confirms that argon has essentially no effect on the coulombic efficiency. In these cases, the SEI is formed solely from ionic liquid components. An increase in coulombic efficiency was seen when the cell was purged with oxygen or nitrogen. Dry air, being mainly a mixture of nitrogen and oxygen, also showed an improvement, however, dry air contains a small amount of carbon dioxide. When the cell was purged with carbon dioxide, a pronounced decrease in coulombic efficiency was observed.

SEM observation of deposited samples showed no major differences in the surface structure of the lithium. Samples were characterized by mossy and dendritic growth, as expected from previous work.[27,28] The main difference between the samples here should be the SEI layer formed to passivate the lithium surface. ToF SIMS was used to sputter into the sample and an elemental depth profile of the SEI and sample was created.

Figure 5 shows a typical depth profile of a lithium sample deposited under Argon. Normalized counts are plotted vs the sputtering time, which is generally proportional to sample depth, assuming uniform sputtering efficiency between the different layers on the lithium

surface. The sensitivity factor for each species was not determined so that an exact mole fraction of each material cannot be calculated. The SEI is clearly observed as a layer of LiF on the surface extending to ~60 s depth, where depth is expressed as a sputtering time. During the course of the experiment, Li^+ and Li_2^+ signals increase indicating bulk lithium has been reached. Li_2^+ represents a lithium cluster peak that appears when the bulk Li deposit has been reached. This makes it a good indicator for the SEI thickness. The Li_2O peak was not tracked because it overlaps with a prominent surface species distorting the results. Instead, the LiO peak is shown. LiO is a natural biproduct of Li_2O during ion bombardment and shows the expected trends. Peaks for Li_3N and LiOH were also tracked and do not appear in significant quantities. When saturated with argon, the SEI is is primarily composed of a LiF layer on the surface.

Depth profiles of samples when the ionic liquid was saturated with dry air, oxygen and nitrogen are shown in Figure 6. Each profile shows a dominate LiF peak at the surface with Li_2 increasing after a decrease in LiF. Surprisingly, Li_3N and LiO were absent from all profiles in Figure 6 even though they are possible reaction products produced between lithium and nitrogen or oxygen. Chemically, the SEI appears to remain a layer of LiF regardless of absorbed gas. This behavior is consistent with the fact that lithium reacts quickly with humid air but lithium is relatively unreactive in dry air. The thermogravimetric analysis by Markowitz et al. shows no weight gain under dry gas, thus no reaction was observed with lithium metal.[29,30] In addition to the slow reaction with nitrogen or oxygen under dry conditions, the gases are present in the ionic liquid at relatively small concentrations compared to the concentration of the ionic liquid components. Thus, LiF formation due to reaction between lithium and the ionic liquid is favored. The SEI composed primarily of LiF layer would then provide surface passivation.

There appears to be a significant difference is in the thickness of the SEI layer formed under the different ambient gases used. Under argon, the thickness of the SEI corresponded to 60 s sputtering time and the coulombic efficiency was 75%. For oxygen and nitrogen, the coubombic efficiency was 86% and the thickness of the SEI corresponded to 20 s of sputtering time. Finally, under dry air, and coulombic efficiency was 83% and it took 150 s to sputter through the SEI. The coulombic efficiency appears to correlate with the coulombic efficiency, except for dry air. Dry air has a coulombic efficiency near nitrogen and oxygen, but an SEI thickness close to the argon sample. The apparent inconsistency with dry air may be explained by the presence of carbon dioxide. Carbon dioxide was quite detrimental to the coulombic efficiency. A depth profile of the SEI formed in carbon dioxide ambient, Figure 7, has a relatively thick layer of LiF, requiring 250 s sputtering time to reach the lithium. In addition, there was no rise of Li_2 as seen in other profiles. When the experiment was conducted in carbon dioxide ambient, bulk lithium deposition was inhibited and a large amount of LiF was produced.

Of the gases tested, carbon dioxide formed the thickest SEI. According to Condemarin et al., Henry's constant for carbon dioxide is 60 atm, while oxygen and nitrogen were not detectable.[22] No data was found for argon solubility. Tf_2N-based ionic liquids have the highest affinity for CO_2 regardless of cation.[26,31] Separation of the anion and cation was observed at high CO_2 pressures.[32] Thus, the association of CO_2 with Tf_2N^- seems to inhibit lithium ion reduction and allow direct electrolyte reduction and degradation. The salt, $LiTf_2N$, could also be affected by the presence of carbon dioxide.

In an attempt to quantify the amount of SEI formed on each sample, two methods were used to estimate the SEI thickness. First, the SIMS depth profiles were converted to depth assuming the materials here sputter at the same rate as a standard material. The sputter rate of gold was

experimentally measured at the same sputtering conditions used in the lithium experiments and found to be 5.2 nm/s. Gold was chosen because it has a molecular weight-to-density ratio similar to lithium, which is a determining factor in sputter rate. The time to sputter through the SEI was determined from the SIMS depth profile and converted to thickness. Second, the SEI thickness was calculated assuming that LIF formation is the sole cause of the loss in coulombic efficiency. The theoretical LiF thickness was calculated by assuming that all lost charge in the cycling experiments (i.e. all lost lithium) went to form LiF instead of metallic Li. By assuming a bulk density for LiF, a thickness can be calculated. The results of these two methods are shown in Table I. The SEI thickness correlates very well with the loss of efficiency. A thinner SEI leads to a higher efficiency, lending credibility to the second method for calculating SEI thickness.

For the argon, nitrogen, and oxygen samples, the two thickness approximations shown in Table 1 are in reasonable agreement. Given that lithium deposits are uneven by their nature and the deposit itself not evenly distributed, the calculated and experimental thicknesses are similar. For carbon dioxide however, the second method, loss of coulombic efficiency, gave a smaller value compared to the sputtering rate measurement. This could be due to a difference in density of the LiF formed when carbon dioxide is present, which could change the sputter rate. Considering the lack of bulk lithium formed, as evidenced by the low Li_2 peak, it is more likely that higher molecular weight reaction products are present in the SEI layer. Peaks for the fragments of the N_{1114} cation were found throughout the carbon dioxide depth profile suggesting an increased breakdown of the ionic liquid; however, the presence of residual ionic liquid on the surface complicates may complicate the analysis. Another possibility is that some of the LiF formed in the carbon dioxide was due to direct reaction between lithium and $LiTf_2N$, rather than

the electrochemical reduction of the salt. The association of Tf_2N^- with carbon dioxide may destabilize the salt causing additional, non-electrochemical side reactions.

Conclusion

Lithium metal deposition and reoxidation was studied under different gas atmospheres in an attempt to evaluate the SEI formed. Cycling experiments were conducted to determine the efficiency of a lithium metal anode under these conditions. SIMS depth profiling was performed on samples deposited under the same conditions to analyze the SEI layer formed. Nitrogen and oxygen atmospheres showed higher coulombic efficiency compared to argon. An experiment under vacuum confirmed that argon does not affect the SEI formation. Carbon dioxide had a detrimental effect on cycling efficiency.

The chemical make-up of the SEI was similar regardless of atmosphere, consisting of mainly of LiF. A correlation between the thickness of the SEI and cycling efficiency was found. It has possible that the lower efficiency comes from the active material and charge lost through formation of the SEI. The SEI layer thickness in carbon dioxide ambient does not correlate as well as the other gases. Carbon dioxide associates strongly with the Tf_2N^- and likely destabilizes the ionic liquid and salt causing other side reactions.

Acknowledgements:

The authors gratefully acknowledge the financial support of the US Army, contract US001-0000335973.

FIGURES

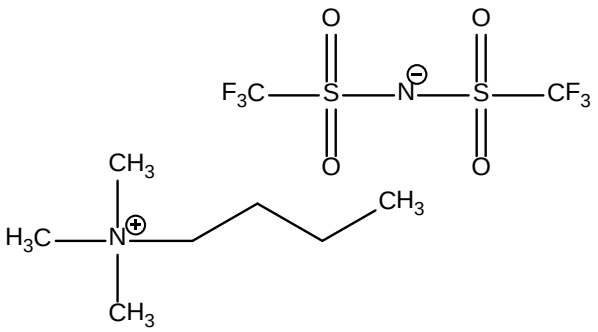

Figure 1. Structure of N_{1114}-Tf_2N ionic liquid. The corresponding salt, Li Tf_2N, was used in the electrolyte.

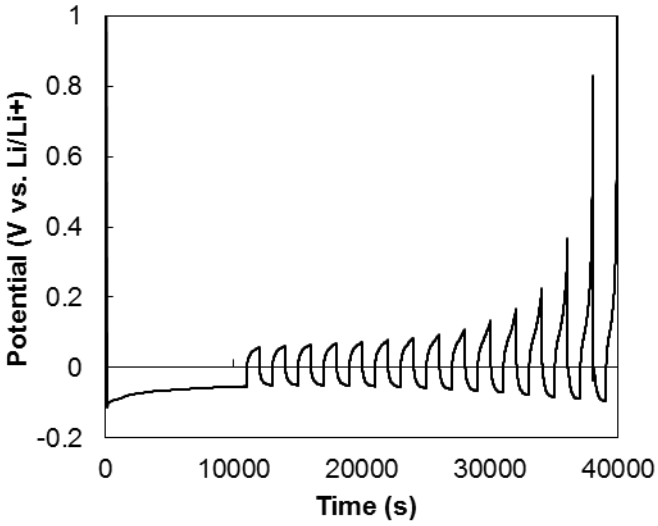

Figure 2. A typical voltage profile recorded under a CO_2 atmosphere. Initially, an excess of lithium was deposited. Then, the cell is cycled until the excess was depleted. An overall efficiency was calculated by summing the combined cathodic and anodic charge.

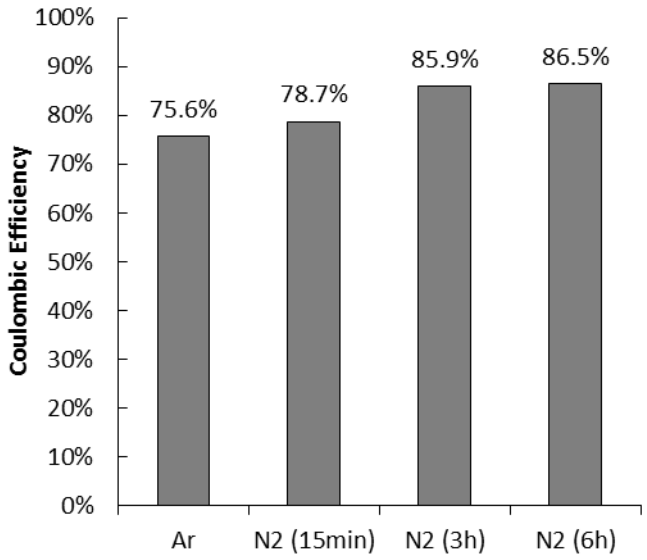

Figure 3. Coulombic efficiency plotted for argon and different gas nitrogen bubbling times.

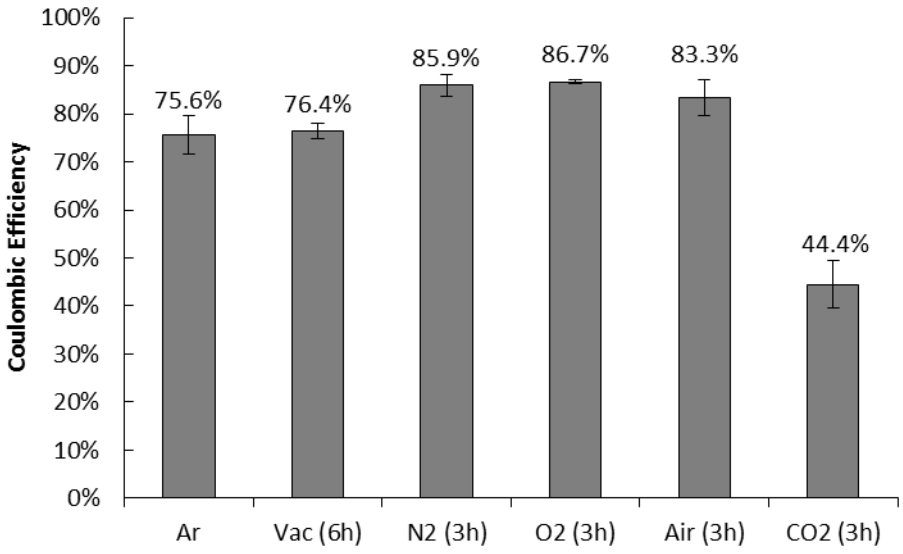

Figure 4. Coulombic efficiency for a lithium anode in ionic liquid bubbled with different gases.

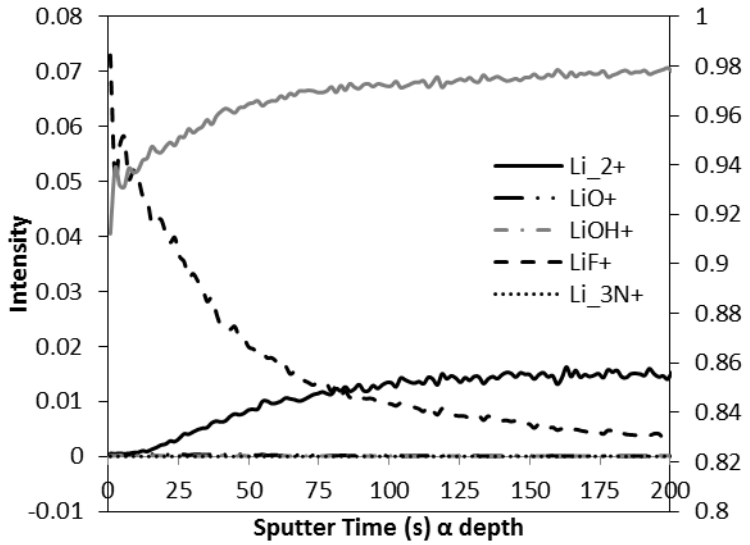

Figure 5. SIMS depth profile of sample deposited under argon atmosphere.

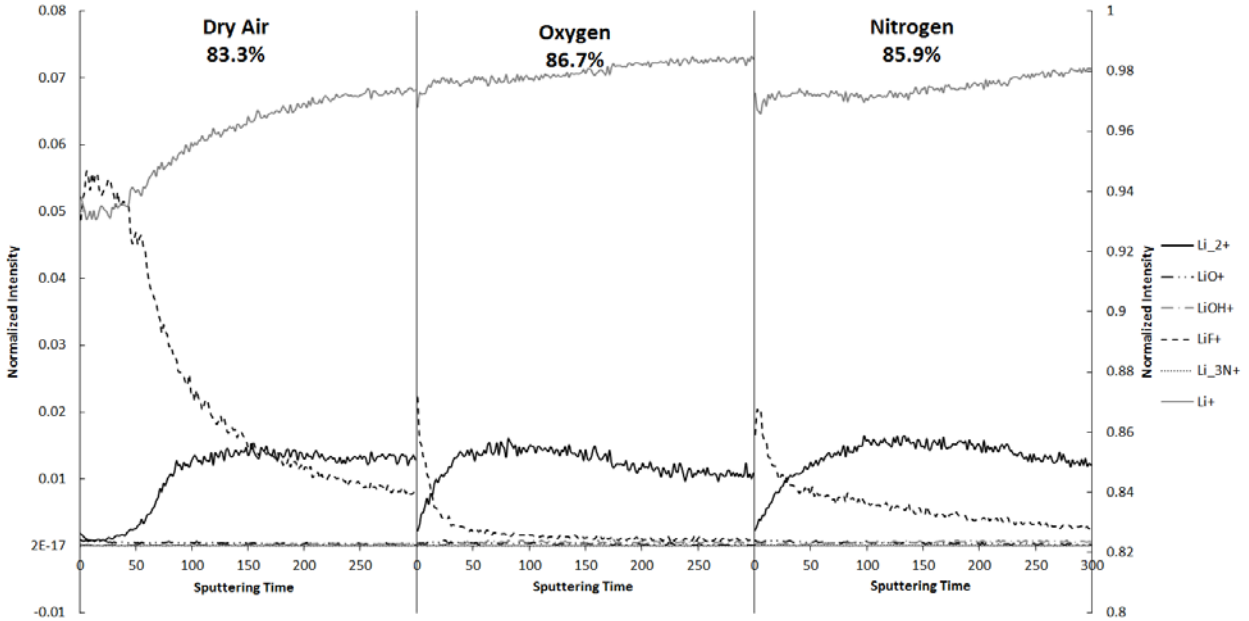

Figure 6. SIMS depth profiles for lithium samples deposited under nitrogen, oxygen and dry air.

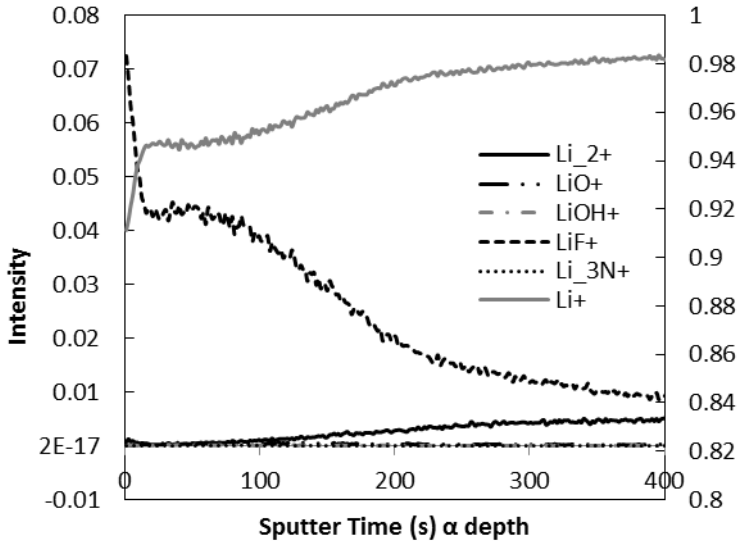

Figure 7. SIMS depth profile of sample deposited in carbon dioxide ambient.

TABLES

	Ar (75%)	N_2/O_2 (85%)	CO_2 (44%)
Thickness based on Au sputter rate	312 nm	104 nm	1300 nm
Thickness calculated from coulombic efficiency	255 nm	152 nm	570 nm

Table I. Comparison of SEI thicknesseses based on SIMS and efficiency calculations.

ACKNOWLEDGEMENTS

The authors gratefully acknowledge the financial support of the US Army, contract US001-0000245070.

REFERENCES

(1) Hirai, T.; Yoshimatsu, I.; Yamaki, J. **1994**, *141*, 611–614.

(2) Zhang, W.-J. *Journal of Power Sources* **2011**, *196*, 13–24.

(3) Zhuang, G. V.; Xu, K.; Jow, T. R.; Ross, P. N. *Electrochemical and Solid-State Letters* **2004**, *7*, A224–A227.

(4) Edström, K.; Herstedt, M.; Abraham, D. P. *Journal of Power Sources* **2006**, *153*, 380–384.

(5) Zheng, H.; Jiang, K.; Abe, T.; Ogumi, Z. *Carbon* **2006**, *44*, 203–210.

(6) Lewandowski, A.; Świderska-Mocek, A. *Journal of Power Sources* **2009**, *194*, 601–609.

(7) Xu, K.; Zhuang, G. V; Allen, J. L.; Lee, U.; Zhang, S. S.; Ross, P. N.; Jow, T. R. *The journal of physical chemistry. B* **2006**, *110*, 7708–7719.

(8) Stark, J. K.; Ding, Y.; Kohl, P. a. *Journal of The Electrochemical Society* **2011**, *158*, A1100–A1105.

(9) Ota, H.; Sakata, Y.; Otake, Y.; Shima, K.; Ue, M.; Yamaki, J. *Journal of The Electrochemical Society* **2004**, *151*, A1778–A1788.

(10) Morigaki, K. *Journal of Power Sources* **2002**, *104*, 13–23.

(11) Momma, T.; Nara, H.; Yamagami, S.; Tatsumi, C.; Osaka, T. *Journal of Power Sources* **2011**, *196*, 6483–6487.

(12) Kim, G.-T.; Jeong, S. S.; Xue, M.-Z.; Balducci, a.; Winter, M.; Passerini, S.; Alessandrini, F.; Appetecchi, G. B. *Journal of Power Sources* **2012**, *199*, 239–246.

(13) Yun, Y. S.; Song, S.-W.; Lee, S.-Y.; Kim, S.-H.; Kim, D.-W. *Current Applied Physics* **2010**, *10*, e97–e100.

(14) Wang, X.; Yasukawa, E.; Kasuya, S. *Journal of The Electrochemical Society* **2000**, *147*, 2421.

(15) Yang, L.; Smith, C.; Patrissi, C.; Schumacher, C. R.; Lucht, B. L. *Journal of Power Sources* **2008**, *185*, 1359–1366.

(16) Crowther, O.; West, A. C. *Journal of The Electrochemical Society* **2008**, *155*, A806.

(17) Wibowo, R.; Aldous, L.; Jones, S. E. W.; Compton, R. G. *Chemical Physics Letters* **2010**, *492*, 276–280.

(18) Stark, J. K.; Ding, Y.; Kohl, P. a. *Journal of The Electrochemical Society* **2011**, *158*, A1100.

(19) Howlett, P. C.; MacFarlane, D. R.; Hollenkamp, A. F. *Electrochemical and Solid-State Letters* **2004**, *7*, A97–A101.

(20) Shimamura, O.; Yoshimoto, N.; Matsumoto, M.; Egashia, M.; Morita, M. *Journal of Power Sources* **2011**, *196*, 1586–1588.

(21) Sakaebe, H.; Matsumoto, H.; Tatsumi, K. *Electrochimica Acta* **2007**, *53*, 1048–1054.

(22) Condemarin, R.; Scovazzo, P. *Chemical Engineering Journal* **2009**, *147*, 51–57.

(23) Ramdin, M.; Loos, T. W. De; Vlugt, T. J. H. *Industrial & Engineering Chemistry Research* **2012**, *51*, 8149–8177.

(24) Blath, J.; Christ, M.; Deubler, N.; Hirth, T.; Schiestel, T. *Chemical Engineering Journal* **2011**, *172*, 167–176.

(25) Anthony, J. L.; Maginn, E. J.; Brennecke, J. F. *Journal of Physical Chemistry B* **2002**, *106*, 7315–7320.

(26) Anthony, J. L.; Anderson, J. L.; Maginn, E. J.; Brennecke, J. F. *Journal of Physical Chemistry B* **2005**, *109*, 6366–7634.

(27) Gireaud, L.; Grugeon, S.; Laruelle, S.; Yrieix, B.; Tarascon, J.-M. *Electrochemistry Communications* **2006**, *8*, 1639–1649.

(28) López, C. M.; Vaughey, J. T.; Dees, D. W. *Journal of The Electrochemical Society* **2009**, *156*, A726–A729.

(29) Markowitz, M.; Boryta, D. *Journal of Chemical and Egineering Data* **1962**, *7*, 586–591.

(30) Rhein, R. A. *Lithium Combustion : A Review by*; 1990; pp. 1–60.

(31) Sharma, P.; Park, S. Do; Baek, I. H.; Park, K. T.; Yoon, Y. I.; Jeong, S. K. *Fuel Processing Technology* **2012**, *100*, 55–62.

(32) Shi, W.; Maginn, E. J. *Journal of Physical Chemistry B* **2008**, *112*, 2045–2055.